Proceedings of the 3rd International Conference on Chemical Engineering (ICCE2021), Mehran University of Engineering and Technology, Jamshoro, September 22-23, 2021, 92-103

Investigation of Methane Combustion under Flameless Conditions through numerical simulations

Munawar Ali Khaskheli[1,*], Masroor Abro[2], Tanweer Hussain[3]

[1] *Energy System Engineering, MUET Jamshoro*

[2] *Chemical Engineering Department, MUET Jamshoro*

[3] *Mechanical Engineering Department, MUET Jamshoro*

[*]*Corresponding Author E-mail: 14PWCHE0910@uetpeshawar.edu.pk*

ABSTRACT

Flameless combustion is a new technology which has several advantages like it works at less temperature which reduces the special metallurgy for the combustor and reduces the chances of generation of NOxs. More work has conducted on the design parameters of combustor particularly on the shape and angle of nozzles. However scant literature is available on the flameless combustion by recirculation of exhaust gases. Moreover, operating parameters like oxygen-to-carbon ratio, fuel feeding rate and fuel temperature were not investigated with exhaust gases recirculation scenario. In present research a model of flameless combustor was developed using commercial CFD software for studying the combustion of methane in flameless conditions. All mentioned important operating parameters were investigated on the developed model. The flameless scenario was created by recirculating the exhaust gases. The partial differential equation of energy, momentum and species were solved numerically. It was observed that the overall temperature of methane combustion was reduced by 20%. Moreover, the NOx generation was also reduced by 25%. The ratio of exhaust mixing with fresh fuel gas played a vital role in flameless combustion.

Keywords:

Methane combustion
Flameless combustion
Exhaust re-circulating injectors
CFD

1. Introduction

Combustion of fossil fuels (e.g., coal, oil, and natural gas) has been the very foundation of the world's industrial society, directly or indirectly generating around 80% (now) and 70% (predicted for 2050) of the total energy for our human life [1-3]. It is unfortunate, however, that burning fossil fuels is also the very major contributor to emissions of both greenhouse gas and ecologically harmful pollutants (e.g., PM2.5, NOx, and SO_2, etc.). Pollutant emissions of combustion derived from energy production and various industry processes must be reduced in the context of an ever-growing energy demand and a heavy dependence upon fossil-fuel combustion in highly capital -intensive infrastructure [4, 5].

Accordingly, over the past five decades or so, extensive research and development (R&D) has been performed to achieve clean and efficient combustion, resulting in substantial reductions in exhaust emissions [6]. However, in practical processes involving combustion, the abatement

of pollutants is often gained at the price of lowering efficiency. That is, many existing main combustion systems are still difficult to operate simultaneously at both high efficiency and low pollution. For example, the staged combustion can significantly reduce emissions of nitric oxides (NOx) by creating the fuel-lean and oxygen-lean combustion regions, but in the same time it decreases the combustion intensity and efficiency [7]. Similarly, the technology of cooling flame [8], which reduces the temperature and thus NOx emissions, may cause combustion instability problems, leading to high emission of carbon monoxide (CO) and hence incomplete combustion. Moreover, applications of the swirl burner4 and the oxy-fuel burner increase the flame temperature, combustion stability, and intensity, but they yield a great deal of pollutants, especially NOx. Also, even with use of various types of low-grade solid fuels and achievement of low NOx emissions, the fluidized bed solid-fuel combustion technologies[8] have to face the problem of relatively low have to face the problem of relatively low combustion efficiency owing to globally low combustion temperature.

To overcome the above drawbacks of the conventional technologies, the moderate or intense low-reactant dilution (MILD) combustion technology or the like have been developed since the early 1990s. Such technologies can concurrently satisfy both needs of high thermal efficiency and low exhaust emissions (e.g., NOx and CO) for application systems [7]. Moderate or intense low-oxygen dilution (MILD) combustion has become a promising low-NOX emission technology, while the delayed mixing of reactants and slower oxidation rate could potentially cause ignition instability in some scenarios [9].

Zharfa and Karimi (2021) [10] numerically investigated the influence of an imposed magnetic field upon the behavior of a reacting flow under hydrogen-methane moderate or intense low oxygen dilution (MILD) regime. This was achieved through addition of a series of baffles close to the inlet nozzles of a well-characterized MILD burner and applying variable intensity magnetic field therein. The simulation results showed that application of the magnetic field allows significant reductions in the air preheating temperature often required for MILD combustion. Xie et al., (2021) [11] proposed a new idea for enhancing the ignition stability for methane MILD combustion by combining with off-stoichiometric combustion (OSC), and assessed its performances numerically through a comparison against the original MILD combustion burner. The results revealed although non-premixed pattern has the lowest NO emission, it suffered from a larger liftoff distance, thus less ignition stability. Si et al., (2021) [12] presented an experimental and numerical study on the moderate or intense low-oxygen dilution (MILD) oxy-combustion characteristics of burning methane in a non-premixed cylindrical furnace. Specifically, the work aimed to investigate the effects of different diluents

(N_2, CO_2, and H_2O) and oxygen concentrations in the oxidant (or the dilution level) on flame stability, combustion, emission, and radiation heat transfer characteristics. Results showed that CO_2 and H_2O dilutions, even for a high oxygen concentration of 30%, were more beneficial than N_2 dilution for realizing the flameless MILD oxy-combustion. Later they developed a new skeletal mechanism of methane MILD combustion by a joint method of Directed Relation Graph (DRG), Computational Singular Perturbation (CSP) and Artificial Neural Network (ANN) (abbreviated as DRG-CSP-ANN method), where DRG and CSP wre used for mechanism reduction and ANN for optimization [13]. The detailed mechanism GRI-3.0, containing 53 species and 325 elementary reactions, was simplified to a skeletal mechanism with only 13 species and 35 reactions, named as Reduced-ANN.

Spatial distributions of temperature, major species and OH mole fractions under MILD conditions in a laminar-jet-in-hot-coflow configuration were measured by Najafi et a., (2021) [14] using spontaneous Raman and laser-induced-fluorescence methods. A preheated mixture of 18% CH_4/82% N_2 at 1100 K was used as fuel, while the products of a laminar, flat, premixed burner-stabilized flame with an equivalence ratio of 0.8 at 1550 K were used as the oxidizer. Analysis of the data shows that the maximum axial and radial temperature and OH mole fraction occur on the lean side of the stoichiometric mixture fraction. Mousavi et al., (2021) [15] numerically investigated the effects of plasma injection upon MILD combustion of a mixture of methane and hydrogen. The results showed that among all the constitutes of plasma, CH_3 is the most effective in improving the characteristics of MILD combustion. Kuang et al., (2021) [16] numerically simulated the pulverized coal MILD combustion with different inlet velocities and oxygen concentrations for its better understanding. Results showed that the oxygen concentration had a more pronounced impact on the chemical reaction, and the inlet velocity had a more pronounced impact on the flow time scale.

Flameless combustion is a new technology which has several advantages like it works at less temperature which reduces the special metallurgy for the combustor, and also reduces the chances of generation of NOxs. More work has conducted on the design parameters of combustor particularly on the shape and angle of nozzles. However scant literature is available on the flameless combustion by recirculation of exhaust gases. Moreover, operating parameters like oxygen-to-carbon ratio, fuel feeding rate and fuel temperature were not investigated with exhaust gases recirculation scenario. Present research aims to develop a flameless combustor for study the combustion of methane in flames less conditions. All mentioned important operating parameters will be investigated on the developed model.

2. CFD model development

Computational fluid dynamics (CFD) modeling is a robust and easy way to investigate complicated engineering systems by solving concerned governing differential equations (GDE) over a computational domain (meshed geometry). There are usually three steps to solve any CFD problem. In the first step the CAD model used to be developed and then it is meshed. In the second step the selected GDEs will be solved numerically. Finally, the results would be extracted in the form of contours diagrams, xy-plots and quantitative reports. The steps of geometry building, meshing and selection of concerned GDEs are discussed in following paragraphs.

2.1. Geometry of flameless combustor

CFD model was developed using commercial CFD software Ansys FLUENT®19.0. The 3D geometry of flameless combustor was developed with the help of Ansys DesignModeler using exhaust re-circulating injectors as shown in Fig. 01. The meshing of the developed geometry was created in Ansys Meshing (Fig 02). The dimensional information and mesh characteristics are shown in Table 01. Overall orthogonal quality of mesh was calculated about 0.524 which shows a reasonable mesh for the numerical computations.

Table 01: Dimensional Information of Geometry and Mesh Characteristics

Sr. No	Parameter	Value
1	Combustor Height	1000 mm
2	Combustor Diameter	600 mm
3	Exhaust diameter	52 mm
4	Diameter of recirculation pipes	30 mm
5	Fuel inlet diameter	20 mm
6	Air inlet	20 mm
7	Type of Mesh	Tetrahedron
8	Mesh size	5,46,628
9	Quality of Mesh (orthogonal)	0.524

2.2. Governing Differential Equations

The present case is of turbulent reacting flow case hence mass continuity, momentum (flow) and energy equations were selected along with species transport equations. The finite rate model was used to define the stoichiometry of the reactions. Five species were used in the

simulations i.e., CH_4, O_2, N_2, CO_2 and H_2O. To handle the turbulence in the flow, standard k-ε model was used. This is a combustion case and high temperature is expected hence, to calculate the radiative heat transfer P-1 radiation model was used. All the selected equations are mentioned in Table 02.

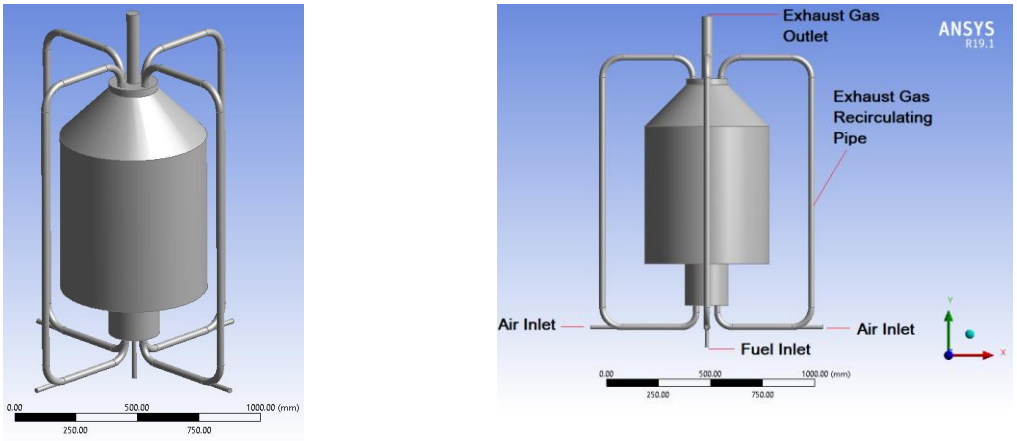

Fig. 01: Different views of flameless combustor with exhaust gas recirculation injectors

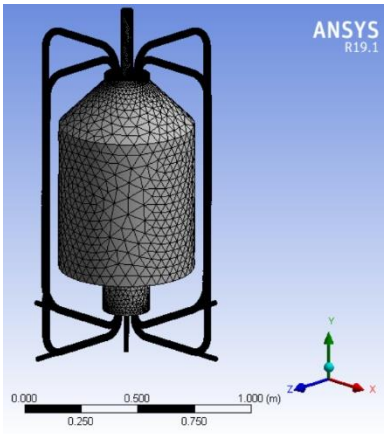

Fig. 02: Meshed geometry

The methane combustion stoichiometry is given in Eq. (8) whereas the equation for calculating equivalence ratio (ϕ) is given in Eq. (9).

$$CH_4 + 2O_2 \rightarrow CO_2 + 2H_2O \quad (1)$$

$$\emptyset = \frac{\left(\frac{Air}{Fuel}\right)_{Stoichiometric}}{\left(\frac{Air}{Fuel}\right)_{Actual}} \quad (2)$$

2.3. Setup of different simulated cases

In present research, total 12 cases were simulated in two groups. In the first group, 8 simulation cases were solved using varying air flowrate (0.0122 kg/sec to 0.0244 kg/sec) which ultimately

vary the equivalence ratio from ϕ=1.426 (lean oxygen environment) to ϕ=0.713 (rich oxygen environment).

Table 02: The selected governing differential equations

Equation Description	**Equation**	**Eq. No.**
Mass	$\nabla.(\rho\vec{v}) = S_m$	(3)
Momentum	$\nabla.(\rho\vec{v}\vec{v}) = -\nabla p + \nabla.(\bar{\bar{\tau}}) + \rho + \vec{F}$	(4)
Specie Equation	$\frac{\partial}{\partial t}(\rho Y_i) + \nabla.(\rho\vec{v}Y_i) = -\nabla.\vec{J_i} + R_i$	(5)
	$\frac{\partial}{\partial t}(\rho k) + \frac{\partial}{\partial x_i}(\rho k u_i) = \frac{\partial}{\partial x_j}\left[\left(\mu + \frac{\mu_t}{\sigma_k}\right)\frac{\partial k}{\partial x_j}\right] + G_k - G_b - \rho\varepsilon - Y_M + S_k$	(6)
Turbulence Model (k-ε)	$\frac{\partial}{\partial t}(\rho\varepsilon) + \frac{\partial}{\partial x_i}(\rho\varepsilon u_i) = \frac{\partial}{\partial x_j}\left[\left(\mu + \frac{\mu_t}{\sigma_\varepsilon}\right)\frac{\partial \varepsilon}{\partial x_j}\right] + C_{1\varepsilon}\frac{\varepsilon}{k}(G_k + C_{3\varepsilon}G_b) - C_{2\varepsilon}\rho\frac{\varepsilon^2}{k} + S_\varepsilon$	(7)
Energy	$\frac{\partial}{\partial x_i}(\rho c_p u_i T) = \frac{\partial}{\partial x_i}\left(\lambda\frac{\partial T}{\partial x_i} - \rho c_p\overline{u_i'T'}\right) + \mu\Phi + S_h$	(8)
Radiation Model (P-1)	$-\nabla q_r = aG - 4aG\sigma a^4$	(9)

In these cases the fuel (CH_4) feed rate was fixed at 0.001 Kg/sec. In the second group of simulations, fuel feed rate was varied from 0.001 to 0.004 Kg/sec at fixed stochiometric equivalence ratio (ϕ=1). The information regarding varying and fixed variables in all simulation cases is highlighted in Table 03.

3. Results and discussion

Numerical simulations were performed to investigate the overall performance of flameless combustor with exhaust recirculating injectors using Ansys FLUENT. The results in terms of temperature of chamber and exhaust flue gases, fuel conversion and flue gas analysis were extracted. The results are discussed in following sub-sections.

Table 03: Conditions of Feed streams for Various Simulated Cases

Sr No	Case Name	Group	Fuel Feed Rate	O2 (Stoi)	Air (Stoi)	% Ex. Air	Excess Air Feed	EQ. Ratio (ϕ)
			Kg/sec	Kg/sec	Kg/sec		Kg/sec	
1	Case_Eq_1.426		0.001	0.004	0.0174	-30	0.0122	1.426
2	Case_Eq_1.252		0.001	0.004	0.0174	-20	0.0139	1.252
3	Case_Eq_1.108		0.001	0.004	0.0174	-10	0.0157	1.108
4	Case_Eq_1	Group	0.001	0.004	0.0174	0	0.0174	1
5	Case_Eq_0.911	1	0.001	0.004	0.0174	10	0.0191	0.911
6	Case_Eq_0.833		0.001	0.004	0.0174	20	0.0209	0.833
7	Case_Eq_0.77		0.001	0.004	0.0174	30	0.0226	0.77
8	Case_Eq_0.713		0.001	0.004	0.0174	40	0.0244	0.713
9	Case_Flow_0.002		0.002	0.008	0.0348	0	0.0348	1
10	Case_Flow_0.003	Group	0.003	0.012	0.0522	0	0.0522	1
11	Case_Flow_0.004	2	0.004	0.016	0.0696	0	0.0696	1
12	Case_Flow_0.004		0.005	0.02	0.087	0	0.087	1

3.1. Effects of Equivalence Ratio

The temperature of chamber along with flue gases were monitored for all the simulated cases and shown in Fig. 03 against varying equivalence ratio. It was observed that the inside temperature of combustion chamber for all the cases is in the range of 1400 to 1580 K, which is much lower temperature in terms of CH_4 combustion of similar case without re-circulation of exhaust gases. The reason behind this lowered temperature is the impact of recirculated CO_2 injection which is at higher temperature and homogenous the temperature equally throughout the chamber. The temperature of exhausting flue gases is little bit lower as compared to inside chamber temperature. The overall range of temperature of exhaust gases lies between 1223 to 1423 K. The maximum temperature of inside chamber was observed 1573 K at ϕ=0.833 which means when there is 20% excess air.

The temperature contours for all the cases are shown in Fig. 04. The figures shows that the recirculating injection of flue gases has critical impact on the flame formation inside the combustion chamber. It has been observed that lean at ϕ =1 or less than 1 has almost no flame produced with in the chamber.

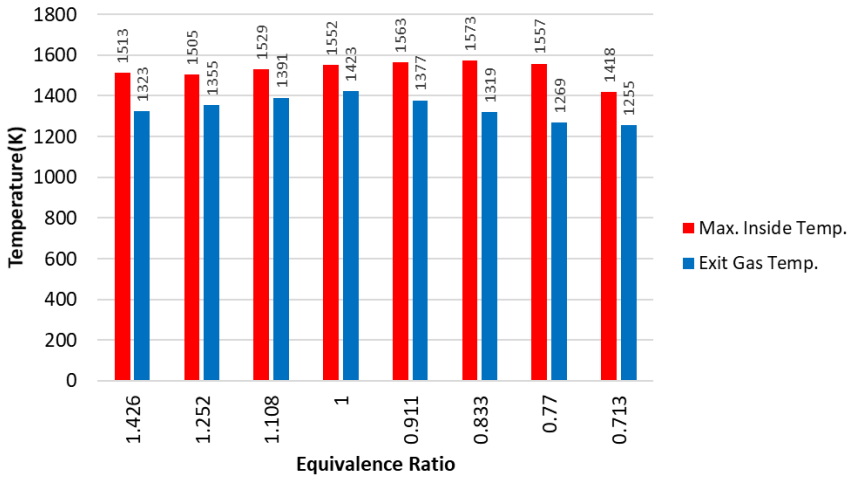

Fig. 03: Temperature of Inside Combustion and Exhaust Flue gases at varying Equivalence Ratio

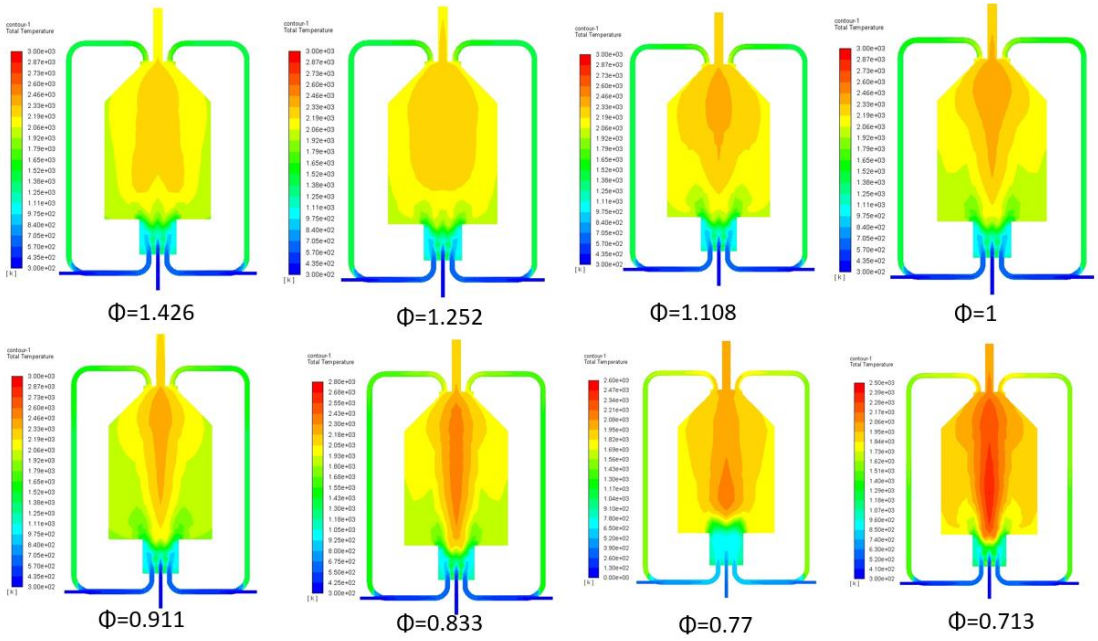

Fig. 04: Temperature contours of inside the combustion chamber for various cases

The conversion of fuel at varying equivalence ratios is shown in Fig. 05. It was observed that at $\phi>1$ (lean oxygen conditions) the conversion is less. The conversion increases with decreasing equivalence ratio (increasing oxygen content in the combustion chamber) and reaches 100% with excess air conditions ($\phi<1$). The conversion is minimum i.e., 69% at $\phi=1.426$ and it is about 98.3% at stoichiometric conditions ($\phi=1$).

The flue gases composition is shown in Fig. 06. From the figure it is has observed that due to low conversion at high equivalence ratios, the unburnt methane is shown in the flue gases.

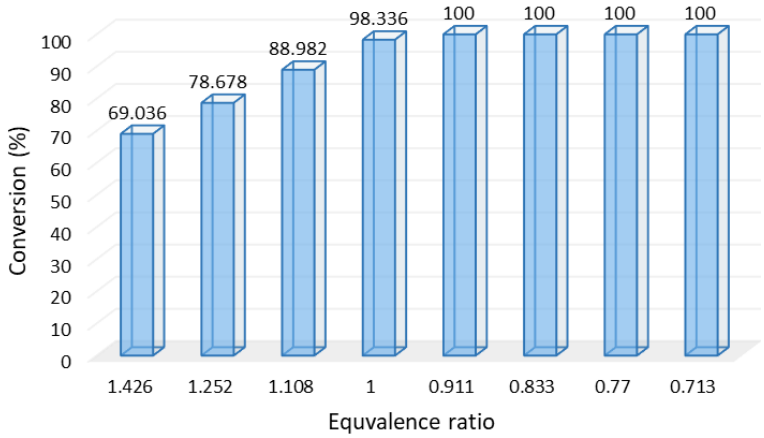

Fig. 05: Conversion of fuel at varying equivalence ratios

However, the in the lower equivalence ratios the CO_2 and H_2O mole fraction is lower due to higher fractions of N_2 with the higher amount of excess air.

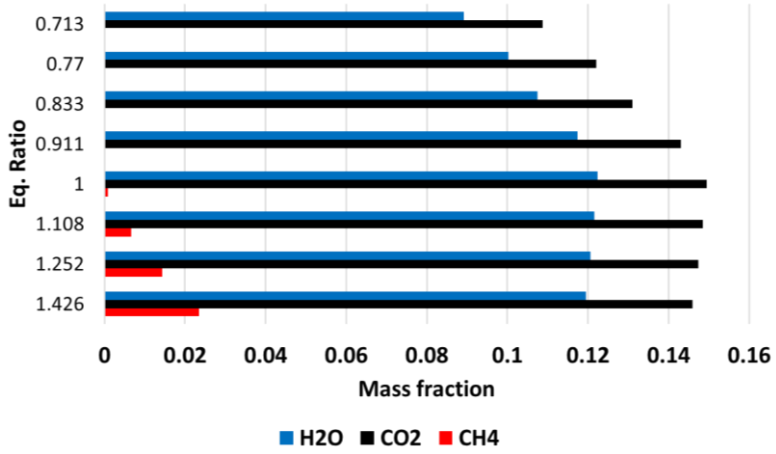

Fig. 06: Composition of flue gases at varying equivalence ratios

3.2. Effect of Feed flowrate

The effect of flowrate of fuel at constant equivalence ratio (ϕ=1) on the temperature of chamber inside and flue gases is shown in Fig. 07. From the figure it has observed that increasing fuel flowrate increases the overall temperature both inside the chamber as well as exhaust flue gases. The maximum temperature of inside chamber was observed 1572 K and for exhaust gases the maximum temperature was observed 1490 K at 0.005 Kg/sec feed flowrate of methane.

The conversion at varying methane flowrate is shown in Fig. 08. It has observed that conversion slightly increases with increasing methane flowrate. Maximum conversion 99.744% was observed at 0.004 Kg/sec methane flowrate. Almost no significant effect was observed as per Fig. 09 in the flue gases composition due to same equivalence ratio at all feed flowrate cases.

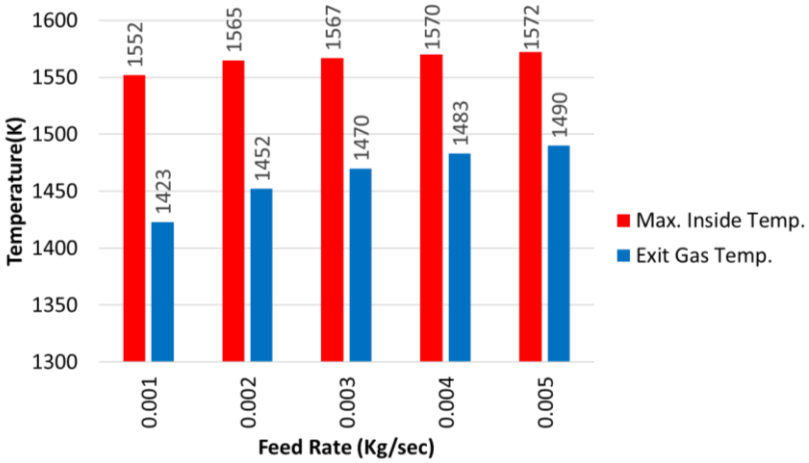

Fig. 07: Temperature of Inside Combustion and Exhaust Flue gases at varying fuel feed flowrate

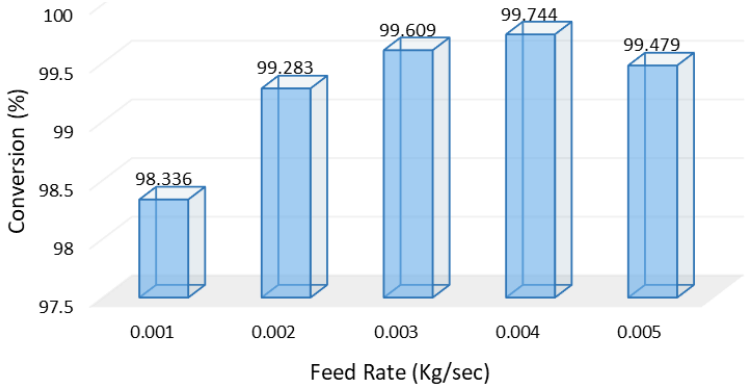

Fig. 08: Conversion of fuel at varying feed flowrate

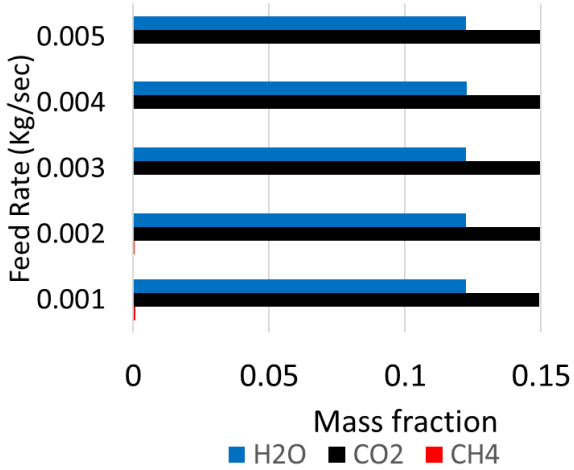

Fig. 09: Composition of flue gases at varying methane flowrate

4. Conclusion

The flameless combustor was simulated numerically with exhaust gases recirculation for methane combustion. Effect of equivalence ratios and fuel feed flowrate was investigated. It is concluded that the simulated flameless combustor showed less temperatures inside the chamber

as compared to conventional combustors due to exhaust recirculation mechanism. Equivalence Ratio had great impact on the conversion of the fuel. At, the maximum conversion (100%) achieved. The minimum conversion (69%) was seen at Φ=1.426. The maximum inside temperature (1557K) was seen at Φ=0.77. Temperature contour diagrams showed the disappearance of flame (high temperature) at inside the chamber. Flue gas analysis showed the unburnt fuel (CH4) at higher equivalence ratios. Increasing feed flowrate at fixed feed temperature showed a slight increase in conversion at Φ=1. Overall, it is concluded that the exhaust recirculation mechanism has capability to achieve Flameless scenario with methane combustion.

In future, few more fuels like hydrogen or hydrocarbon fuels could be tested in future with same geometry. The transient simulations could also be developed to study dynamic behavior of combustor. Reaction kinetics could be studied for flameless combustion. The work could also be extended for experimental verifications for the simulated scenarios. NOx could be calculated in future studies.

References

5. Mi, J. and *et al.*. Review on MILD Combustion of Gaseous Fuel: Its Definition, Ignition, Evolution, and Emissions. *Energy & Fuels*, 2021. 35(9): P. 7572-607.
6. Si, J. and *et al.*. Optimization of the Global Reaction Mechanism for MILD Combustion of Methane Using Artificial Neural Network. *Energy & Fuels*, 2020. 34(3): P. 3805-15.
7. Tu, Y. and *et al.*. Numerical study of methane combustion under moderate or intense low-oxygen dilution regime at elevated pressure conditions up to 8 atm. *Energy*, 2020. 197: P. 117158.
8. Wang, G. and *et al.*. MILD combustion versus conventional bluff-body flame of a premixed CH4/air jet in hot coflow. *Energy*, 2019. 187: P. 115934.
9. Zhang, Z. and *et al.*. Numerical investigation of the effects of different injection parameters on Damköhler number in the natural gas MILD combustion. *Fuel*, 2019. 237: P. 60-70.
10. Mardani, A and *et al.*. Numerical assessment of MILD combustion enhancement through plasma actuator. *Energy*, 2019. 183: P. 172-84.
11. Cavaliere, A., Mild combustion. *Progress in Energy and Combustion science*, 2004. 30(4): P. 329-66.
12. Wünning, J. and *et al.*. Flameless oxidation to reduce thermal NO-formation. *Progress in energy and combustion science*, 1997. 23(1): P. 81-94.

13. Cheong, K-P., and *et al.*. Nonpremixed MILD combustion in a laboratory-scale cylindrical furnace: Occurrence and identification. *Energy*, 2021. 216: P. 119295.
14. Zharfa, M. and *et al.*. Intensification of MILD combustion of methane and hydrogen blend by the application of a magnetic field- a numerical study. *Acta Astronautica,* 2021. 184: P. 259-68.
15. Xie, M. and *et al.*. A numerical study of accelerated moderate or intense low-oxygen dilution (MILD) combustion stability for methane in a lab-scale furnace by off-stoichiometric combustion technology. *Chinese Journal of Chemical Engineering*, 2021. 32: P. 108-18.
16. Si, J. and *et al.*. Experimental and Numerical Study on Moderate or Intense Low-Oxygen Dilution Oxy-Combustion of Methane in a Laboratory-Scale Furnace under N_2, CO_2, and H_2O Dilutions. *Energy & Fuels*, 2021. 35(15): P. 12403-15.
17. Si, J. and *et al.*. A new skeletal mechanism for simulating MILD combustion optimized using Artificial Neural Network. *Energy*, 2021. 237: P. 121603.
18. Najafi, SBN. and *et al.*. and *et al.*. (Non)Equilibrium of OH and Differential Transport in MILD Combustion: Measured and Computed OH Fractions in a Laminar Methane/Nitrogen Jet in Hot Coflow. *Energy & Fuels*, 2021. 35(8): P. 6798-806.
19. Mousavi, S. M. and *et al.*. Numerical Investigation of the Plasma-Assisted MILD Combustion of a CH4/H2 Fuel Blend Under Various Working Conditions. *Journal of Energy Resources Technology*, 2021. 143(6).
20. Kuang, Y. and *et al.*. Flow and reaction characteristics at different oxygen concentrations and inlet velocities in pulverized coal MILD combustion. *Journal of the Energy Institute*, 2021. 94: P. 63-72.